Earth And Planetary Science Letters
May 2021, Volume 562 Pages 116840 (12p.)
https://doi.org/10.1016/j.epsl.2021.116840
https://archimer.ifremer.fr/doc/00683/79478/

Mass 47 clumped isotope signatures in modern lacustrine authigenic carbonates in Western China and other regions and implications for paleotemperature and paleoelevation reconstructions

Li Huashu [1] , Liu Xingqi [1], Arnold Alexandrea [2], Elliott Ben [2], Flores Randy [2], Kelley Anne Marie [2], Tripati Aradhna [2, 3, 4]

[1] College of Resource Environment and Tourism, Capital Normal University, 100048 Beijing, PR China
[2] Department of Earth, Planetary, and Space Sciences, Department of Atmospheric and Oceanic Sciences, Institute of the Environment and Sustainability, Center for Diverse Leadership in Science, University of California, Los Angeles, CA 90095, USA
[3] European Institute of Marine Sciences (IUEM), Université de Brest, UMR 6538, Domaines Océaniques, Rue Dumont D'Urville, 29280 Plouzané, France
[4] IFREMER, Laboratoire Géophysique et enregistrement Sédimentaire, 29280 Plouzané, France

Email addresses : lihuashu525@sina.com ; xqliu@cnu.edu.cn ; ajarnold1@ucla.edu ; benm.elliott@epss.ucla.edu ; randyjflores@gmail.com ; panter2dobey@ucla.edu ; atripati@g.ucla.edu

Abstract :

With the development of the carbonate clumped isotope () geothermometer, many –temperature calibrations based on biogenic and abiogenic carbonates have been generated in recent years. However, there is still not a robust empirical calibration relationship derived from lacustrine authigenic carbonates that can be used to calculate lake water temperatures from values. In this study, we present a new calibration dataset that is comprised of measurements of the clumped isotope composition of 33 lacustrine authigenic carbonates collected from terminal lakes primarily in Western China that cover a substantial altitudinal gradient, and 5 samples from other regions. These data allow us to directly derive a temperature calibration for lacustrine authigenic carbonates. Our results show a robust correlation between modern lacustrine authigenic carbonate clumped isotope composition (Δ47carb) values and independently measured mean summer water surface temperatures (Twater) (ranging from 9.8 to 26.0 °C), which confirms the utility of mass-47 clumped isotope measurements of lacustrine authigenic carbonates as a lake water temperature indicator and allows for the derivation of the following calibration equation: Δ47carb (‰) = 0.0521 ± 0.0071 × 106/ (K) + 0.0904 ± 0.0870 (R2 = 0.6224, P < 0.0001, n = 33). We observe that Δ47carb is significantly correlated to lake elevation at 35°N from 270 to 5,156 m a.s.l. The change in –derived water temperature differences through elevation gradients (i.e. lapse rate) is around 3.2 °C/km. We do not observe a significant correlation between Δ47carb and carbonate oxygen isotopic composition or independently measured lake surface water oxygen isotopic composition. Additionally, in our dataset, we find that water chemistry, carbonate precipitation rate, carbonate content and mineral-specific differences do not significantly affect Δ47carb values. Hence, the mass-47 clumped isotope signal

of lacustrine authigenic carbonate can be used in paleotemperature and paleoaltimetry studies if post-depositional diagenesis did not modify the isotopic composition.

Highlights

► Lacustrine authigenic carbonate Δ_{47} is correlated with summer water temperature. ► Δ_{47carb} isn't affected by δ 18O of carbonate and lake water. ► Δ_{47carb} is independent of carbonate content, mineralogy, and precipitation rate. ► The Δ_{47carb}-elevation calibration improves the use of Δ_{47carb} for paleoaltimetry. ► We provide a robust basis for reconstructions of paleoclimate using Δ_{47carb}.

Keywords : clumped isotope, lacustrine authigenic carbonate, paleotemperature reconstruction, paleoclimate, paleoaltimetry

1. Introduction

Lacustrine carbonates are widely distributed and highly sensitive to changes in water source and terrestrial environment (Leng and Marshall, 2004). In general, lacustrine carbonates precipitate in summer, when the carbonate saturation of lake water peaks and carbonate solubility is simultaneously depressed in the epilimnion (Horton et al., 2016; Hren and Sheldon, 2012; Leng and Marshall, 2004; Petryshyn et al., 2015). In the carbonate-water system, at equilibrium, the oxygen isotopic composition of carbonate is a function of the temperature of carbonate precipitation and surrounding water oxygen isotope ratios (McCrea, 1950; Urey, 1947). Therefore, oxygen isotopic fractionations between lacustrine carbonates and water are widely used to estimate lake water temperature in paleolimnology studies (Finkenbinder et al., 2016; Ibarra et al., 2014).

However, there are several limitations for the application of carbonate oxygen isotope geothermometer in lake settings. For example, the oxygen isotopic composition of lake waters for geologic samples is often difficult to constrain. Prior work relies on an assumption of the lake water oxygen isotopes or numerical modeling (Benson and Paillet, 2002; Leng and Marshall, 2004). Non-equilibrium fractionation effects due to changes in solution chemistry and carbonate precipitation processes, and mineral-specific difference might also affect the oxygen isotope fractionation factor between carbonates and surrounding waters (Kim et al., 2007; Watkins and Hunt, 2015). In addition, some field studies show that the oxygen isotopic compositions of lacustrine carbonates are largely influenced by rainfall or

local precipitation/evaporation balance, rather than temperature changes (Li et al., 2020; Liu et al., 2018; Sun et al., 2018). All of these limitations increase the uncertainty of temperature reconstructions based on carbonate oxygen isotope geothermometer in paleoenvironmental studies.

The mass-47 carbonate clumped isotope (Δ_{47}) geothermometer represents a promising tool for reconstructing paleotemperature (Eiler, 2007; Ghosh et al., 2006a; Tripati et al., 2010; Tripati et al., 2015). Quantitative temperature estimates that are independent from water $^{18}O/^{16}O$ ratios is the most important feature that distinguishes carbonate clumped isotope thermometer from the carbonate oxygen isotopic thermometer and other approaches. The clumped isotope composition is defined as the excess of the abundance of $^{13}C–^{18}O$ bonds in a carbonate lattice over the expected stochastic distribution among all isotopologues of CO_2. Under thermodynamic equilibrium, the preference of ^{13}C and ^{18}O bonding is thermodynamically controlled and is independent of the bulk isotopic composition of the carbonate and the solution in which the carbonate formed (Eiler, 2007; Hill et al., 2020; Hill et al., 2014; Tripati et al., 2015).

An initial Δ_{47}–temperature calibration was published by Ghosh et al. (2006a) based on inorganic calcites precipitated at controlled temperatures as well as deep-sea and tropical surface corals. In the last 14 years, multiple studies have discussed the applicability of biogenic and abiogenic carbonate clumped isotope thermometers, and a variety of theoretical and empirical calibrations were published (Davies and John, 2019; Eagle et al., 2013a; Guo et al., 2009; Kele et al., 2015; Kelson et al., 2017;

Petersen et al., 2019; Thiagarajan et al., 2011; Tripati et al., 2010; Zaarur et al., 2011). However, recent studies show statistically significant discrepancies between Δ_{47}–temperature calibrations derived from different laboratories which have been attributed to lack of sample replication, the narrow temperature range of different types of carbonate materials (Fernandez et al., 2017), non-equilibrium processes caused by pH effects (Hill et al., 2014; Tripati et al., 2015), CO_2 diffusion (Thiagarajan et al., 2011), hydration/dehydration and hydroxylation/dehydroxylation reactions (Guo et al., 2008), or inconsistent correction schemes, such as ^{17}O correction and acid digestion temperature and standardization (Bernasconi et al., 2018; Dennis et al., 2011; Kelson et al., 2017).

There are almost no clumped isotope-temperature data or calibration datasets for modern lake systems, and controls on mass-47 fractionations in specific types of lacustrine carbonates have not been investigated in detail. The first clumped isotope study of modern lake carbonates was reported by Huntington et al. (2010), who measured Δ_{47} values of micrites and tufa from six modern lakes on the Colorado Plateau. This study calculated carbonate precipitation temperatures using the Ghosh calibration (Ghosh et al., 2006a), and applied the differences in Δ_{47}-derived temperatures between ancient and modern samples at several elevations to reconstruct paleoelevations. Petryshyn et al. (2015) measured modern lake microbialites and reported evidence that carbonate precipitation was in equilibrium, and that Δ_{47}-derived calcification temperature of shallow microbialites matched current lake water temperatures if an inorganic calibration was used. In addition, they also

reconstructed past lake water temperatures using ancient microbialites. Huntington et al. (2014) reported that Δ_{47}-derived temperatures of shallow-water tufa that collected from Ngangla Ring Tso are similar to warm-season lake water temperatures, and used clumped data to study the Miocene and Pliocene uplift history of Zhada Basin. Additionally, several studies have estimated lake water $\delta^{18}O$ values based on lacustrine carbonate Δ_{47}-derived temperatures along with carbonate $\delta^{18}O$ values and $\delta^{18}O$ fractionation factor between carbonate and surrounding water (Horton et al., 2016; Petryshyn et al., 2015), and reconstructed lake level in the past (Yang et al., 2019).

Although clumped isotope compositions of different types of lacustrine carbonates have been applied to reconstruct paleoclimate and paleoelevation, all previous studies have calculated Δ_{47}-derived water temperature using synthetic carbonate calibrations (Hudson et al., 2017; Huntington et al., 2010). Given that lacustrine systems and carbonate precipitation processes are complex, there is a need for studies that systematically explore how reliable lacustrine authigenic carbonate Δ_{47} measurements reflect lake water temperature, and how robust the empirical Δ_{47}-temperature relationship is for different types of carbonates in natural settings. Therefore, systematic analyses of natural lacustrine authigenic carbonates with well-constrained carbonate growth temperatures, and a more comprehensive carbonate Δ_{47}–temperature calibration which span a wider range of carbonate precipitation temperatures, are essential for the accurate interpretation of lacustrine carbonate mass-47 measurements as a proxy.

In this study, we collected lacustrine authigenic carbonates from 33 terminal lakes primarily from Western China that range in elevation and temperature, a region that is of interest for both paleoaltimetry and paleoclimate. For each site, we measured the clumped and bulk isotopic compositions of carbonate samples and independently measured lake water temperatures. We also include an additional dataset with measurements of 5 calcite micrite samples collected from closed/dry lakes in China, the United States and Mexico, and independently derived water temperatures to further explore the Δ_{47}-temperature relationship (Mering, 2015), processed in accordance with best practices for clumped isotope reporting (Defliese and Tripati, 2020; Petersen et al., 2019). The goals of this study were to investigate: (1) whether there is a statistically significant correlation between lacustrine authigenic carbonate Δ_{47} values and lake water temperatures; (2) whether Δ_{47} values in modern lacustrine authigenic carbonates are independent of the oxygen isotope composition of carbonate and water, and not influenced by water chemistry, carbonate precipitation rates or carbonate mineralogy; (3) whether the temperature sensitivity of Δ_{47} values in lacustrine authigenic carbonate is in agreement with other type of carbonates; (4) whether lacustrine authigenic carbonate Δ_{47} can be used in paleotemperature and paleoelevation studies.

2. Study regions and hydrographic data sources

Information about the 33 samples from China is discussed here, while site information and data for the 5 samples from other regions are discussed in a thesis

(Mering, 2015).

2.1. Study regions

Western China is considered a semi-arid and arid region, characterized by low, uneven rainfall and high evaporation (Yang et al., 2011). There are a large number of natural lakes distributed throughout the region, which account for roughly 58.3% of the quantity and 66.9% of the area of all Chinese lakes (Ma et al., 2011). Due to the influence and limitations of complicated geological formations and natural environments, most of the lakes are terminal lakes with relatively high-salinity, oligotrophic and cool water, the population density of phytoplankton is relatively low, and the microbial bloom is weak or concentrated within a short time in these lakes (Liu et al., 2008; Wen et al., 2005). Based on the large differences of geographical locations, basin topography, local climates, and hydrological conditions, these lakes are sensitive to environmental changes, especially to variations in temperature (Greve et al., 2018).

2.2. Samples

Thirty-three lakes were selected for this study cover a large environmental gradient in China, over a geographical range of 29.2 to 47.1°N and 81.2 to 116.5°E (Fig. 1). The elevation (Elev) of lakes sampled for this study ranges from 270 to 5,156 m (a.s.l.).

Lake surface sediment samples were collected in the field in July and August

2016. To ensure that the samples were not influenced by hydrological or human disturbance, sediment samples were collected at the center of the lake for smaller lakes and at least 2 km away from the shore for larger lakes. In each lake, the top 0.5 cm of surface sediments were collected using a stainless grab and were placed in leak proof plastic bags. All samples were stored in a cooler in the field and were then stored at 4℃ in Capital Normal University, China.

3. Analytical methods

3.1. Water surface temperature collection

HOBO U22 Water Temperature Pro v2 data loggers (manufacturer's accuracy of ± 0.2℃) were set 50 cm under the water surface for each lake during July and August 2016. Water temperature data was collected at 15-minute intervals over the course of one year. Twelve data loggers were successfully retrieved the following summer; however, the rest of the loggers were lost. Midday temporal water temperature (T_{MTW}) was also manually measured using a mercurial thermometer (manufacturer's accuracy of ± 0.5℃) at 50 cm under the water surface in the same location of water sampling in 2016. T_{MTW} was measured once for each lake at roughly 2 p.m., during the warmest time of day, when the sediment and water samples were collected and when authigenic carbonate precipitation is most likely to occur in this region (Hren and Sheldon, 2012).

3.2. Lake surface sediment samples pretreatments

Samples were soaked in deionized water for 2 hours and then wet sieved with a 350-mesh (45 μm) sieve. Materials exceeding 45-μm containing detrital fragments and biogenic carbonates (containing primarily ostracods) were filtered out, and the fine fraction carbonates smaller than 45 μm were characterized as the authigenic carbonate which were chemically precipitated in lake water (Zhai et al., 2015; Zhang et al., 2016). The remaining fine-sieved fractions were collected and poured into centrifuge tubes and centrifuged for approximately 5 minutes (3000 r/min). The dilution was decanted and the sediment samples were placed in leak proof plastic bags. These samples were frozen in a refrigerator overnight and then vacuum freeze-dried for 48 hours using the Boyikang FD-1A-50 Freeze Dryer at approximately −50 °C (30 Pa), until the samples were dried. Around 2 g of each sieved sediment sample was ground using agate mortar and pestle and stored in a desiccator prior to analysis.

3.3. Stable and clumped isotope measurements

Samples were treated with 3% hydrogen peroxide for 4 hours to remove organic material (Eagle et al., 2013b). Following treatment, samples were collected on a 0.45 μm cellulose nitrate filter membrane and oven-dried at 40℃, a temperature sufficiently low to prevent bond reordering (Passey and Henkes, 2012; Stolper and Eiler, 2015; Swart et al., 2016). Depending on carbonate content and instrument sensitivity at the time of analysis, the amount of sample weighed into silver capsules for analysis varied between 12 and 95 mg.

Stable and clumped isotopes were measured with a Thermo Scientific MAT 253

gas source isotope mass spectrometer in the Tripati Laboratory at the University of California, Los Angeles, USA from 2017 to 2018. Samples were reacted with 105% phosphoric acid (ρ = 1.92 g/mL) for 20 minutes on a 90°C online common phosphoric acid bath system to convert to CO_2 gas for analyses. Acid temperature was monitored with a thermocouple throughout each analysis and checked daily for drift. The phosphoric acid was changed every 10 to 15 analyses. The liberated CO_2 was successively passed through a dry ice/ethanol trap (−76°C) and a liquid nitrogen trap (−196°C) to remove water and other compounds. After the initial purification step, the CO_2 was passed through silver wool to remove sulfur compounds and then passed through a Porapak Q gas chromatograph column at −20°C to remove any additional contaminants before being transferred into the bellows of the mass spectrometer for analysis. Data were collected over 9 acquisition cycles to determine $\delta^{13}C$, $\delta^{18}O$, Δ_{47}, Δ_{48}, and Δ_{49}. At least three replicates per sample were performed.

Sample isotope compositions were measured against a high purity pre-calibrated CO_2 tank as the reference gas (From 1/19/2017 to 2/21/2018: Air Liquide with $\delta^{18}O$ = 19.31‰ VSMOW, $\delta^{13}C$ = −3.38‰ VPDB; after 2/21/2018: Oztech with $\delta^{18}O$ = −15.84 ‰ VPDB, $\delta^{13}C$ = −3.64‰ VPDB), whose composition has been determined through comparison with NBS standard gases and CO_2 evolved by acid digestion from NBS-19 and NBS-18. During analysis, carbonate standards, including NBS-19 and ETH-1 through 4 were analyzed between every 2-3 samples.

For all samples, including from Mering (2015) that were measured in the Tripati laboratory at UCLA, we processed raw mass spectrometer data using the software

program *Easotope* (John and Bowen, 2016), and corrected ^{17}O using IUPAC (International Union of Pure and Applied Chemistry) parameters (Brand et al., 2010) as recommended by Daëron et al. (2016). We corrected for non-linearity in the mass spectrometer by using two equilibrated gas standards with different bulk compositions, half of which were heated to 1000℃ for two hours and then quenched at room temperatures to represent a stochastic distribution, and the other half were equilibrated with water at 25℃. We converted all clumped isotope measurements into the Absolute Reference Frame (ARF) (Dennis et al., 2011) using a suite of carbonate standards, with values defined by Bernasconi et al. (2018). We also applied an acid digestion fractionation factor of 0.082‰ (Defliese et al., 2015) to derive clumped isotope data relative to the stochastic distribution in order to compare with previous published carbonate data which are digested in phosphoric acid at 25℃. Replicates with elevated Δ_{48} or Δ_{49} values that differed from carbonate standards, indicating contamination, or anomalous Δ_{47}, $\delta^{13}C$ and $\delta^{18}O$ values indicative of contamination by water or incomplete digestion were excluded in this study (Tripati et al., 2015).

4. Results

4.1. Lake water and surface sediment information

4.1.1. Summer water surface temperature

Lacustrine authigenic carbonate precipitation occurs primarily during summer (Hren and Sheldon, 2012; Leng and Marshall, 2004), mean summer water surface temperatures are used in this study. Logged mean summer water temperature (T_{LMSW})

from June to August was calculated using the data recorded by the on-site loggers retrieved from twelve lakes. A linear regression was established based on twelve T_{LMSW} and corresponding T_{MTW} measured by mercurial thermometer in the field (Fig. 2):

$$T_{LMSW} = 1.19 \pm 0.09 T_{MTW} - 4.43 \pm 1.61 \ (n = 12, R^2 = 0.91, P < 0.0001) \quad (1)$$

For the sites where water temperature loggers were lost in the field, we determined the calculated mean summer water temperature (T_{CMSW}) by applying regression (1) to the T_{MTW} values for the lakes without loggers. Thus, in this study, lake summer water surface temperature (T_{water}) is either T_{LMSW} (lakes with loggers) or T_{CMSW} (lakes without loggers). T_{water} ranged from 9.8 to 26.0℃ (Table A. 1).

4.1.2. Mineralogy and isotopic composition of modern lacustrine authigenic carbonates

XRD analyses show that there are 9 pure calcite samples and 24 mixed mineralogy samples for modern lacustrine authigenic carbonates in this study. For most samples, calcite and aragonite are the dominant carbonate species, with limited dolomite content (Li et al., 2020). The mixed mineralogy samples are divided into 9 calcite-dominated samples, 3 monohydrocalcite-dominated samples and 12 aragonite-dominated samples based on mineral content.

For most modern lacustrine authigenic carbonate samples, 3 to 6 replicates were analyzed for $\delta^{13}C$, $\delta^{18}O$, and Δ_{47}. No Δ_{47} value is reported for carbonates collected from 5 lakes (Daihai Lake, Dali Lake, Jinzihai Lake, Hurleg Lake, and Bosten Lake)

because of high Δ_{48}, Δ_{49} values or anomalous values of Δ_{47}, $\delta^{13}C$ and $\delta^{18}O$, which indicate organic contaminations or incomplete digestion.

The average Δ_{47} values of 28 modern lacustrine authigenic carbonates (Δ_{47carb}) range from 0.670 to 0.761‰ (Table A. 2). Reproducibility of Δ_{47carb} for most samples within the typical standard error on replicate analyses of 0.01‰. Weighted mean modern authigenic lacustrine carbonate oxygen isotope composition ($\delta^{18}O_{carb}$) range from −9.61 to 3.77‰ (VPDB) (Li et al., 2020).

4.2. Correlation of mass-47 with temperature

In order to maximize data population and the range of temperatures covered by the calibration, we combine our Δ_{47} values from 28 modern lacustrine authigenic carbonates in China and 5 modern micrite samples collected from closed/dry lakes from Mering (2015), which were measured on the same instrument using the same methodology and reprocessed using the same parameters. The average Δ_{47carb} values are plotted versus lake mean summer water temperatures expressed as $10^6/T^2_{water}$ (Fig. 3). A linear least-squares regression yields the following relationship:

$$\Delta_{47carb}\ (‰) = 0.0521 \pm 0.0071 \times 10^6/T^2_{water}\ (K) + 0.0904 \pm 0.0870\ (R^2 = 0.6224,\ P < 0.0001,\ n = 33) \quad (2)$$

It is evident that Δ_{47carb} values generally increase with decreasing T_{water} range included in this study. Individual samples fit well within the error of the regression, supporting the validity of the lacustrine authigenic carbonate calibration.

5. Discussion

5.1. Clumped isotope fractionation in modern lacustrine authigenic carbonates

The use of clumped isotopes as a geothermometer implicitly assumes equilibrium isotopic fractionation (Eiler, 2007). Prior work has constrained equilibrium ^{13}C–^{18}O compositions within dissolved inorganic carbonate species and in carbonate minerals (Tripati et al., 2015), as well as theoretically explored dependence on growth rate (Watkins and Hunt, 2015). More recent work has suggested disequilibrium may be more prevalent in carbonates (Daëron et al., 2019). Our previous work (Li et al., 2020) presented disequilibrium oxygen isotope fractionations in lacustrine authigenic carbonates from the same sites examined in this study, and attributed the $\delta^{18}O$ departure from expected values to lake water pH and carbonate precipitation rate-related effects. However, we see that Δ_{47carb} values exhibit a significant linear correlation with independently measured T_{water} (Fig. 3). No significant correlation is observed between Δ_{47carb} and $\delta^{18}O_{carb}$, nor is there a correlation between Δ_{47carb} and independently measured $\delta^{18}O_{water}$ for modern lacustrine authigenic carbonates (Fig. 4a and b). Thus, we conclude that the ^{13}C–^{18}O bond ordering in modern lacustrine carbonates are independent of oxygen isotopic compositions of carbonate and lake water in this study.

5.1.1. Influence of solution chemistry

Theoretical calculations and laboratory experiments suggest that solution pH and salinity can affect carbonate Δ_{47} values through dissolved inorganic carbonate (DIC)

speciation (Hill et al., 2014; Tripati et al., 2015). Each DIC species has a distinct clumped isotope composition for a given temperature (Guo et al., 2008; Hill et al., 2014). Δ_{47} values between HCO_3^- and CO_3^{2-} at 25°C have been reported to differ by 0.033‰ to 0.063‰ (Hill et al., 2014; Tripati et al., 2015). The distribution of DIC species is pH-dependent, and the Δ_{47} value of the DIC pool decreases when solution pH changes from an intermediate range (HCO_3^- dominant) to a high range (CO_3^{2-} dominant) (Watkins and Hunt, 2015). In addition, salinity is also observed to influence DIC speciation by changing ions and ion pairing (Millero et al., 2006). Thus, an increase in solution pH or decrease in salinity lowers the Δ_{47} value of DIC pool at a given temperature (Hill et al., 2014; Tripati et al., 2015). However, pH and salinity are only expected to influence carbonate Δ_{47} when carbonate mineral grows rapidly from a mixture of DIC species, thus, it may not have sufficient time to reach equilibrium and will inherit signatures from the DIC pool (Watkins and Hunt, 2015). Kelson et al. (2017) explored pH effects on Δ_{47} values of synthetic carbonates precipitated in a wide range of temperatures and found no significant pH-induced effects on Δ_{47} values over a range of experimental carbonate growth rates.

In this study, the water salinity of the sites sampled ranged from 0.35 to 87.99 g/L, while pH ranges from 7.89 to 9.81, with HCO_3^- the dominant DIC species in a majority of these lakes (Li et al., 2020). We investigated pH-related speciation effects by comparing the deviation of measured from expected $\delta^{18}O_{carb}$ ($\Delta(\delta^{18}O_{carb})$) to Δ_{47carb} ($\Delta(\Delta_{47carb})$). The expected $\delta^{18}O_{carb}$ values are calculated using the equation defined by Kim and O'Neil (1997) based on $\delta^{18}O_{carb}$ and independently measured T_{water} in this

study. The predicted Δ_{47carb} values are calculated using the recalculated Kele et al. (2015) calibration (Bernasconi et al., 2018) based on independently measured T_{water} in this study. As shown in Fig. 5, the correlation between $\Delta(\delta^{18}O_{carb})$ and $\Delta(\Delta_{47carb})$ is not significant. The $\Delta(\Delta_{47carb})$-$\Delta(\delta^{18}O_{carb})$ slope of regression through modern lacustrine authigenic carbonates ($m = 0.0017 \pm 0.0012$) is not consistent with a pH effect that observed in synthetic witherites ($m = 0.011 \pm 0.001$) or cultured corals ($m = 0.010 \pm 0.03$) (Tripati et al., 2015). In addition, we find that Δ_{47carb} is not significantly correlated with changes in lake water salinity (Fig. 6). Therefore, our results suggest that solution chemistry does not significantly affect Δ_{47} signal of lacustrine authigenic carbonates, which is similar to what has been reported for cultured mollusks (Eagle et al., 2013a), foraminifera (Tripati et al., 2010) and travertines (Kele et al., 2015). This is consistent with the findings of Tripati et al. (2015) that potential Δ_{47} offsets caused by combined changing pH and salinity during Last Glacial Maximum and Cenozoic would be negligible for tropical marine carbonates.

5.1.2. Influence of precipitation rate

Carbonate precipitation rate has also been suggested as a potential factor modulating kinetic fractionations in Δ_{47} (Watkins and Hunt, 2015). The precipitation rate of lake surface sediment ranges from 0.01 cm/year to 0.3 cm/year in different lakes in this study (Yan and Wunnemann, 2014; Zhou et al., 2007). Although determining the exact precipitation rates of lacustrine authigenic carbonates can be challenging, the carbonate growth rates in this study are consistent with other reports

404 in natural settings, which is similar to or relatively lower than those laboratory
405 synthetic carbonates (Karami et al., 2019; Tang et al., 2014). Tang et al. (2014) found
406 increases in carbonate precipitation rate cause slight decreases in $\delta^{18}O$ but do not
407 influence Δ_{47} values of synthetic inorganic calcites within measurement precision.
408 According to the process based on the model of Watkins and Hunt (2015), the
409 difference in Δ_{47} between calcite in slow-growth and fast-growth regimes at 25°C is
410 only around 0.01‰ at pH values between 8 and 10. Therefore, the lack of a pH effect
411 observed in this study indicates that the growth rates of modern lacustrine authigenic
412 carbonates may not be sufficiently high for DIC speciation effects to be recorded in
413 Δ_{47}. Even if pH or rate related Δ_{47} disequilibrium occurs in this study, it may be within
414 analytical uncertainties and can be neglected (Kelson et al., 2017; Tang et al., 2014).
415
416 **5.1.3. Influence of mineral-specific differences and carbonate content**
417 Small mineral-specific differences in clumped isotopic fractionation are
418 predicted by Guo et al. (2009), Tripati et al. (2015), and Hill et al. (2020). Most
419 studies have not been able to discern significant mineral-specific Δ_{47} offsets
420 (Bonifacie et al., 2017; Davies and John, 2019; Defliese et al., 2015; Eagle et al., 2010;
421 Guo et al., 2019; Petersen et al., 2019), though some work has suggested otherwise
422 (Müller et al., 2019). In this study, 22 samples are a mixture of two or three types of
423 carbonate minerals, with calcite and aragonite being the predominant species in most
424 samples (Table A. 2). We applied a two-sample Kolmogorov-Smirnov test (Massey,
425 1951) for Δ_{47carb} values of calcite-dominated and aragonite-dominated samples. Our

results indicate that the compositional differences between calcite-dominated and aragonite-dominated samples are not statistically significative (D-value = 0.4549; P = 0.0712). As shown in Figures 3 to 6, no significant Δ_{47} inconsistency is observed among samples with different mineral compositions. Therefore, Δ_{47} offsets caused by differences mineral species can be neglected in this study. This result is also supported by a compiled dataset reprocessed by Petersen et al. (2019) that presented no statistically Δ_{47} discrepancy between different carbonate mineralogies.

In order to discuss the influence of carbonate content, we evaluated the deviation of measured lacustrine authigenic carbonate Δ_{47} (Δ_{47carb}) values from theoretical calculations. We calculated theoretical Δ_{47} ($\Delta_{47calculated}$) values by applying the latest "universal" clumped isotope calibration (Petersen et al., 2019) to independently measured water temperatures (T_{water}) of the 28 lakes in China from this study. There is a significant correlation ($R^2 = 0.5028$, $P < 0.0001$) between Δ_{47carb} and $\Delta_{47calculated}$ (Fig. 7(a)), and the RMSE of Δ_{47carb} versus $\Delta_{47calculated}$ is 0.0143. As shown in the Fig. 7(b), the Δ_{47} residual does not decrease with increasing carbonate content. The correlation between Δ_{47} residual and carbonate content is not significant ($R^2 = 0.00118$, P = 0.8682). This suggests that an influence from carbonate content on Δ_{47carb} values can be neglected.

As a result, we presume that at current instrumental resolution, the clumping of ^{13}C and ^{18}O in modern lacustrine authigenic carbonates is not affected by disequilibrium fractionations caused by solution chemistry, carbonate precipitation rate, carbonate content or mineralogy.

448

449 **5.2. Comparison of our Δ_{47}–temperature calibration with other clumped isotope**
450 **calibrations**

451 The temperature dependence of clumped isotope fractionation in our samples and
452 other studies are compared in Fig. 8. In order to allow direct and precise comparisons,
453 in this section, we only choose to compare with datasets that used ETH carbonate
454 standards calculated with IUPAC parameters and are in the ARF.

455 The Δ_{47}–temperature calibration of modern lacustrine authigenic carbonates
456 overall agrees with laboratory synthetic carbonate calibrations and empirically
457 determined calibrations. The results for modern tufa and travertine from natural
458 springs and wells (Kele et al., 2015) recalculated by Bernasconi et al. (2018) fall close
459 to the 95% confidence interval of our calibration line. Analysis of covariance
460 (ANCOVA) results indicate that difference between slopes of our lacustrine
461 authigenic carbonate calibration line and the recalculated Kele et al. (2015) calibration
462 (Bernasconi et al., 2018) is not significant (p = 0.2274). Our calibration line is also
463 closely aligned with the latest "universal" clumped isotope calibration from Petersen
464 et al. (2019), that recalculated published calibration data using consistent parameters.
465 In addition, data points from Devils Hole and Laghetto Basso, which have been
466 suggested to approach true thermodynamic equilibrium in natural settings (Daëron et
467 al., 2019), are also within error of our calibration. The consistency of temperature
468 sensitivity between our results and other calibrations supports the premise that
469 lacustrine authigenic carbonates record Δ_{47} signatures that are close to equilibrium,

and that water temperature is the primary environmental variable controlling lacustrine authigenic carbonate Δ_{47}.

In spite of the good correspondence, slight discrepancies between the slope and intercept of published calibrations remain (Petersen et al., 2019). The development and using of the Absolute Reference Frame (Dennis et al., 2011), IUPAC parameters for ^{17}O correction (Brand et al., 2010), and the use of carbonate standards to project the results to the ARF (Bernasconi et al., 2018) have improved data comparability in different laboratories. Remaining discrepancies between calibration relationships may come from the pinning of carbonate standard values in the Absolute Reference Frame (Defliese et al., 2015), standardization (Kocken et al., 2019; Defliese and Tripati, 2020), differences in sample replication and temperature range of calibrations (Fernandez et al., 2017), and procedures used for sample measurement and data calculation (Olack and Colman, 2019).

5.3. Applications

5.3.1. Applications to study paleoclimate

The clumped isotope thermometer has been used for paleotemperature reconstruction in different regions and over various time scales (Eagle et al., 2013b; Újvári et al., 2019), including in lacustrine carbonates (Frantz et al., 2014; Horton et al., 2016; Petryshyn et al., 2016; Santi et al., 2020). In order to evaluate the accuracy of using lacustrine authigenic carbonate Δ_{47} values to reconstruct water temperatures using our derived Δ_{47}–temperature calibration, we calculated lacustrine authigenic

carbonate clumped isotope temperature ($T_{\Delta47carb}$) by applying the Δ_{47}–temperature calibration (Eq. 2) to the carbonate Δ_{47} values and compare it with independently measured carbonate formation summer water temperatures (T_{water}). As shown in Fig. 9, there is a strong positive correlation between T_{water} and $T_{\Delta47carb}$ in modern lacustrine authigenic carbonates:

$$T_{\Delta47carb}\ (°C) = 1.014 \pm 0.1362 \times T_{water}\ (°C) - 0.1889 \pm 2.318\ (R^2 = 0.6412,\ P < 0.0001,\ n = 33) \quad (3)$$

The slope of the least-squares linear regression line is close to 1, indicating that the Δ_{47}–derived temperature recorded in lacustrine authigenic carbonates has similar temperature sensitivity to actual water temperature. The average standard error is 1.82℃ and the RMSE of $T_{\Delta47carb}$ versus T_{water} is 3.29℃ that within the standard error (0 ~ 4.57℃) in individual sample. Therefore, our empirical Δ_{47}–temperature calibration (Eq. 2) can be used to estimate lake summer water temperatures with reasonable certainty. The scatter of data in this regression may be caused by analytical uncertainties, water temperature measurements, and carbonate precipitation processes.

Our results demonstrate that using Δ_{47} values of modern lacustrine authigenic carbonates to calculate summer water temperatures is reasonable, and that lacustrine authigenic carbonates preserved in geologic archives should also reliably record contemporary water temperatures when carbonate samples are not diagenetically alternated. Although the average $T_{\Delta47carb}$ standard error of 1.8℃ is similar to uncertainties based on other types of carbonate including shallow and deep-dwelling foraminifers (Meinicke et al., 2020), field-collected land snails (Zhai et al., 2019), and

514 modern soil carbonates (Hough et al., 2014), the magnitude of uncertainty is still
515 relatively large. Future study is needed to expand calibration data sets, especially for
516 higher lake water temperatures, and optimize statistical methods used to improve
517 accuracy of predictions.
518
519 **5.3.2. Applications to study paleoelevation**
520 Clumped isotopes can be applied to reconstruct paleoaltimetry in cases where
521 post-depositional diagenesis, which reorders the carbonate clumped isotopic
522 compositions, did not occur (Henkes et al., 2014; Huntington and Lechler, 2015). As
523 Δ_{47} values provide direct measures of carbonate formation temperatures, previous
524 studies have usually combined the estimates of paleotemperature with general surface
525 temperature-elevation gradient (lapse rate) to reconstruct the elevation changes during
526 the past based on the assumption that all temperature changes reflect elevation
527 changes (Ghosh et al., 2006b; Huntington et al., 2010).
528 Lake surface water temperature is mainly controlled by air temperature, which is
529 related to lake latitude and elevation. Other factors, such as wind, water inflow and
530 outflow, and lake volume, may not significantly impact the water temperature changes
531 at lake center over various time scales (Hren and Sheldon, 2012; Zhang et al., 2014).
532 Figure 10 shows a combined effect of both lake latitude (Lat) and elevation (Elev) on
533 lake surface water temperatures (T_{water}) for the 33 lakes we analyzed that are primarily
534 located in Western China:
535 T_{water} (°C) = –0.2869 ± 0.1537 × Lat – 0.0036 ± 5.3236 × 10^{-4}× Elev (m) + 39.1518 ±

536 7.2426 (R^2 = 0.8502, P < 0.0001, n = 33) (4)

537 In order to allow direct and precise comparisons between lacustrine authigenic
538 carbonate clumped isotope composition and lake elevation, the influence from lake
539 latitude on water temperature should be eliminated. To this effect, we recalculated
540 lake elevations based on Equation 4, assuming all lakes are located at 35°N, which is
541 a mean value of the latitude gradient of the 33 lakes investigated in this study. In this
542 case, the vertical transect dominates T_{water} variances and corresponding Δ_{47carb} values.
543 We evaluated the correlation between Δ_{47carb} and recalculated lake elevation as well as
544 between $T_{\Delta47carb}$ and recalculated lake elevation. As shown in Fig. 11, Δ_{47carb} increases
545 simultaneously with lake elevation, while $T_{\Delta47carb}$ decreases with increasing lake
546 elevation:

547 Δ_{47carb} (‰) = $1.359 \times 10^{-5} \pm 2.678 \times 10^{-6} \times$ Elev (m) + 0.6665 ± 0.0103 (R^2 = 0.4975, P
548 < 0.0001, n = 28) (5)

549 $T_{\Delta47carb}$ (°C) = $-3.195 \times 10^{-3} \pm 6.14 \times 10^{-4} \times$ Elev (m) + 27.21 ± 2.363 (R^2 = 0.5101, P
550 < 0.0001, n = 28) (6)

551 Accordingly, the Δ_{47}-derived water temperature lapse rate is around 3.2 °C/km from
552 270 to 5,156 m a.s.l..

553 Lapse rates are not necessarily consistent for different types of materials (i.e., air
554 temperature lapse rates, soil temperature lapse rates, and lake temperature lapse rates),
555 given that heat capacities vary between materials. According to Meyer (2007), the air
556 temperature lapse rate is ~ 6 °C/km. Hren and Sheldon (2012) investigated the
557 relationship between modern lake water temperature and air temperature in different

time scales, and observed a warmest month mean water temperature lapse rate of 3.5 °C/km for low and mid-latitude lakes, which is similar to our results in this study. A recent study by Hough et al. (2014) used soil clumped isotope geothermometer as a proxy in paleoelevation reconstructions of the central Rocky Mountains and found a temperature lapse rate of modern soil is around 4 °C/km. This temperature lapse rate is steeper than what we report for lake water and could reflect the smaller specific heat of soil comparing to water bodies. In addition, the lapse rate of our $T_{\Delta 47carb}$–elevation calibration (Eq. 6) is not as steep as that of Huntington et al. (2010) (4.2 °C/km), which is the first study that focused on modern lacustrine carbonate clumped isotopes collected from the Colorado Plateau; however, we note that Hough et al. (2014) and Huntington et al. (2010) calculated $T_{\Delta 47}$ values using the Ghosh calibration (Ghosh et al., 2006a), which has a steeper Δ_{47}–temperature slope (m = 0.0636) than ours (m = 0.0493) (Eq. 2) and did not directly calculate lapse rates using instrumented data, as we have. The discrepancies in the slopes of Δ_{47}–temperature calibrations are presumably responsible for the difference in the $T_{\Delta 47}$–elevation lapse rates calculated in this study relative to previous publications.

Based on our results, when temperature changes caused by climate evolution can be ruled out, the clumped isotope analysis of lacustrine authigenic carbonates can be applied to estimate elevation changes. As both lake latitude and elevation are predominant factors controlling water temperature, one should consider differences in lake latitude and select a suitable zero elevation temperature or reference temperature (Huntington and Lechler, 2015). Therefore, a site- or regional-specific transfer

function is needed to reconstruct paleoelevation when using lacustrine authigenic carbonate clumped isotopes.

6. Conclusions

This study systematically analyzes the clumped isotope of modern lacustrine carbonates based on a compilation of data from 38 lakes, including 33 terminal lakes primarily in Western China that span a range of elevations. We investigate the correlations between carbonate Δ_{47} values and mean summer water temperatures as well as bulk isotopic compositions. We also investigate the influence of water chemistry, precipitation rates, carbonate content, and mineral-specific differences, and refine the interpretations of carbonate clumped isotope temperature sensitivity.

In our results, the clumping of ^{13}C and ^{18}O in modern lacustrine authigenic carbonates is independent of bulk isotopic compositions of carbonate and surrounding water and is not affected by disequilibrium fractionations caused by water chemistry, carbonate precipitation rate, carbonate content, or mineral-specific differences at current analytical precision. The clumped isotope composition of lacustrine authigenic carbonate is sensitive to summer water temperature changes, and the temperature sensitivity is consistent with other previous studies. We propose a reliable lacustrine authigenic carbonate Δ_{47}–temperature empirical calibration covering the temperature ranges from 9.8 to 26.0°C that can be used in paleotemperature reconstructions: Δ_{47carb} (‰) = 0.0521 ± 0.0071 × $10^6/T^2_{water}$ (K) + 0.0904 ± 0.0870 (R^2 = 0.6224, P < 0.0001, n = 33). Based on the significant positive correlation between lacustrine authigenic

carbonate clumped isotope and lake elevations at 35°N, we suggest that lacustrine authigenic carbonate Δ_{47} can also be used in paleoelevation reconstructions when climate forcing can be constrained using other methods.

Author contribution statement

Huashu Li: Conceptualization, Formal analysis, Investigation, Writing-Original draft preparation, Data Curation, Writing- Reviewing and Editing. **Xingqi Liu**: Conceptualization, Investigation, Writing-Reviewing and Editing, Supervision, Project administration. **Alexandrea Arnold**: Formal analysis, Investigation, Data Curation, Writing-Reviewing and Editing. **Ben Elliott**: Investigation, Resources. **Randy Flores**: Investigation. **Anne Marie Kelley**: Investigation. **Aradhna Tripati**: Investigation, Resources, Data Curation, Writing- Reviewing and Editing, Supervision, Project administration.

Acknowledgments

This work was supported by the National Natural Science Foundation of China (NSFC 41572338), the Second Tibetan Plateau Scientific Expedition and Research Program (STEP) (Grant No. 2019QZKK0202) and a NSF CAREER award (NSF EAR-1352212), with mass spectrometry supported by the Department of Energy through BES grant DE-FG02-13ER16402. All UCLA students were supported by the Center for Diverse Leadership in Science.

Declarations of interest:

None.

Appendix A. Supplementary material

Tables A.1–A.3. The supplementary material contains three data tables, which include lake information and results from the analysis of authigenic carbonates and standards in this study.

References

Benson, L., Paillet, F., 2002. HIBAL: a hydrologic-isotopic-balance model for application to paleolake systems. Quaternary science reviews 21, 1521-1539.

Bernasconi, S.M., Müller, I.A., Bergmann, K.D., Breitenbach, S.F., Fernandez, A., Hodell, D.A., Jaggi, M., Meckler, A.N., Millan, I., Ziegler, M., 2018. Reducing uncertainties in carbonate clumped isotope analysis through consistent carbonate-based standardization. Geochemistry, Geophysics, Geosystems 19, 2895-2914.

Bonifacie, M., Calmels, D., Eiler, J.M., Horita, J., Chaduteau, C., Vasconcelos, C., Agrinier, P., Katz, A., Passey, B.H., Ferry, J.M., 2017. Calibration of the dolomite clumped isotope thermometer from 25 to 350°C, and implications for a universal calibration for all (Ca, Mg, Fe) CO_3 carbonates. Geochimica et Cosmochimica Acta 200, 255-279.

Brand, W.A., Assonov, S.S., Coplen, T.B., 2010. Correction for the ^{17}O interference in δ (^{13}C) measurements when analyzing CO_2 with stable isotope mass spectrometry (IUPAC Technical Report). Pure and Applied Chemistry 82, 1719-1733.

Daëron, M., Blamart, D., Peral, M., Affek, H., 2016. Absolute isotopic abundance ratios and the accuracy of Δ_{47} measurements. Chemical Geology 442, 83-96.

Daëron, M., Drysdale, R.N., Peral, M., Huyghe, D., Blamart, D., Coplen, T.B., Lartaud, F., Zanchetta, G., 2019. Most Earth-surface calcites precipitate out of isotopic equilibrium. Nature communications 10, 429.

Davies, A.J., John, C.M., 2019. The clumped (^{13}C-^{18}O) isotope composition of echinoid calcite: Further evidence for "vital effects" in the clumped isotope proxy. Geochimica et Cosmochimica Acta 245, 172-189.

Defliese, W.F., Hren, M.T., Lohmann, K.C., 2015. Compositional and temperature effects of phosphoric acid fractionation on Δ_{47} analysis and implications for discrepant calibrations. Chemical Geology 396, 51-60.

Defliese, W.F., Tripati, A., 2020. Analytical effects on clumped isotope thermometry: comparison of a common sample set analyzed using multiple instruments, types of standards, and standardization windows. Rapid Communications in Mass Spectrometry 34.

Dennis, K.J., Affek, H.P., Passey, B.H., Schrag, D.P., Eiler, J.M., 2011. Defining an absolute reference frame for 'clumped'isotope studies of CO_2. Geochimica et Cosmochimica Acta 75, 7117-7131.

Eagle, R., Eiler, J.M., Tripati, A.K., Ries, J., Freitas, P., Hiebenthal, C., Wanamaker, A.D., Taviani, M., Elliot, M., Marenssi, S., 2013a. The influence of temperature and seawater carbonate saturation state on ^{13}C–^{18}O bond ordering in bivalve mollusks. Biogeosciences 10, 4591-4606.

Eagle, R.A., Risi, C., Mitchell, J.L., Eiler, J.M., Seibt, U., Neelin, J.D., Li, G., Tripati, A.K., 2013b. High regional climate sensitivity over continental China constrained by glacial-recent changes

668 in temperature and the hydrological cycle. Proceedings of the National Academy of Sciences
669 110, 8813-8818.
670 Eagle, R.A., Schauble, E.A., Tripati, A.K., 2010. Body temperatures of modern and extinct vertebrates
671 from ^{13}C-^{18}O bond abundances in bioapatite. Proceedings of the National Academy of
672 Sciences 107, 10377-10382.
673 Eiler, J.M., 2007. "Clumped-isotope" geochemistry—The study of naturally-occurring,
674 multiply-substituted isotopologues. Earth and planetary science letters 262, 309-327.
675 Fernandez, A., Müller, I.A., Rodríguez-Sanz, L., van Dijk, J., Looser, N., Bernasconi, S.M., 2017. A
676 reassessment of the precision of carbonate clumped isotope measurements: Implications for
677 calibrations and paleoclimate reconstructions. Geochemistry, Geophysics, Geosystems 18,
678 4375-4386.
679 Finkenbinder, M.S., Abbott, M.B., Steinman, B.A., 2016. Holocene climate change in Newfoundland
680 reconstructed using oxygen isotope analysis of lake sediment cores. Global and Planetary
681 Change 143, 251-261.
682 Frantz, C.M., Petryshyn, V.A., Marenco, P.J., Tripati, A., Berelson, W.M., Corsetti, F.A., 2014.
683 Dramatic local environmental change during the Early Eocene Climatic Optimum detected
684 using high resolution chemical analyses of Green River Formation stromatolites.
685 Palaeogeography Palaeoclimatology Palaeoecology 405, 1-15.
686 Ghosh, P., Adkins, J., Affek, H., Balta, B., Guo, W., Schauble, E.A., Schrag, D., Eiler, J.M., 2006a.
687 ^{13}C–^{18}O bonds in carbonate minerals: a new kind of paleothermometer. Geochimica et
688 Cosmochimica Acta 70, 1439-1456.
689 Ghosh, P., Garzione, C.N., Eiler, J.M., 2006b. Rapid uplift of the Altiplano revealed through ^{13}C-^{18}O

bonds in paleosol carbonates. Science 311, 511-515.

Greve, P., Gudmundsson, L., Seneviratne, S.I., 2018. Regional scaling of annual mean precipitation and water availability with global temperature change. Earth System Dynamics 9, 227-240.

Guo, W., Daeron, M., Niles, P., Genty, D., Kim, S.-T., Vonhof, H., Affek, H., Wainer, K., Blamart, D., Eiler, J., 2008. ^{13}C-^{18}O bonds in dissolved inorganic carbon: Implications for carbonate clumped isotope thermometry. Geochimica et Cosmochimica Acta 72, A287-A338.

Guo, W., Mosenfelder, J.L., Goddard III, W.A., Eiler, J.M., 2009. Isotopic fractionations associated with phosphoric acid digestion of carbonate minerals: insights from first-principles theoretical modeling and clumped isotope measurements. Geochimica et Cosmochimica Acta 73, 7203-7225.

Guo, Y., Deng, W., Wei, G., 2019. Kinetic effects during the experimental transition of aragonite to calcite in aqueous solution: Insights from clumped and oxygen isotope signatures. Geochimica et Cosmochimica Acta 248, 210-230.

Henkes, G.A., Passey, B.H., Grossman, E.L., Shenton, B.J., Pérez-Huerta, A., Yancey, T.E., 2014. Temperature limits for preservation of primary calcite clumped isotope paleotemperatures. Geochimica et cosmochimica acta 139, 362-382.

Hill, P.S., Schauble, E.A., Tripati, A., 2020. Theoretical constraints on the effects of added cations on clumped, oxygen, and carbon isotope signatures of dissolved inorganic carbon species and minerals. Geochimica et Cosmochimica Acta 269, 496-539.

Hill, P.S., Tripati, A.K., Schauble, E.A., 2014. Theoretical constraints on the effects of pH, salinity, and temperature on clumped isotope signatures of dissolved inorganic carbon species and precipitating carbonate minerals. Geochimica et cosmochimica acta 125, 610-652.

712 Horton, T.W., Defliese, W.F., Tripati, A.K., Oze, C., 2016. Evaporation induced ^{18}O and ^{13}C enrichment
713 in lake systems: A global perspective on hydrologic balance effects. Quaternary Science
714 Reviews 131, 365-379.
715 Hough, B.G., Fan, M., Passey, B.H., 2014. Calibration of the clumped isotope geothermometer in soil
716 carbonate in Wyoming and Nebraska, USA: Implications for paleoelevation and paleoclimate
717 reconstruction. Earth and Planetary Science Letters 391, 110-120.
718 Hren, M.T., Sheldon, N.D., 2012. Temporal variations in lake water temperature: Paleoenvironmental
719 implications of lake carbonate $\delta^{18}O$ and temperature records. Earth and Planetary Science
720 Letters 337, 77-84.
721 Hudson, A.M., Quade, J., Ali, G., Boyle, D., Bassett, S., Huntington, K.W., Marie, G., Cohen, A.S., Lin,
722 K., Wang, X., 2017. Stable C, O and clumped isotope systematics and ^{14}C geochronology of
723 carbonates from the Quaternary Chewaucan closed-basin lake system, Great Basin, USA:
724 Implications for paleoenvironmental reconstructions using carbonates. Geochimica et
725 Cosmochimica Acta 212, 274-302.
726 Huntington, K., Wernicke, B., Eiler, J., 2010. Influence of climate change and uplift on Colorado
727 Plateau paleotemperatures from carbonate clumped isotope thermometry. Tectonics 29.
728 Huntington, K.W., Lechler, A.R., 2015. Carbonate clumped isotope thermometry in continental
729 tectonics. Tectonophysics 647, 1-20.
730 Huntington, K.W., Saylor, J., Quade, J., Hudson, A.M., 2014. High late Miocene–Pliocene elevation of
731 the Zhada Basin, southwestern Tibetan Plateau, from carbonate clumped isotope thermometry.
732 Geological Society of America Bulletin 127, 181-199.
733 Ibarra, Y., Corsetti, F.A., Cheetham, M.I., Feakins, S.J., 2014. Were fossil spring-associated carbonates

near Zaca Lake, Santa Barbara, California deposited under an ambient or thermal regime? Sedimentary geology 301, 15-25.

John, C.M., Bowen, D., 2016. Community software for challenging isotope analysis: First applications of 'Easotope' to clumped isotopes. Rapid Communications in Mass Spectrometry 30, 2285-2300.

Karami, F., Balci, N., Guven, B., 2019. A modeling approach for calcium carbonate precipitation in a hypersaline environment: A case study from a shallow, alkaline lake. Ecological Complexity 39, 100774.

Kele, S., Breitenbach, S.F., Capezzuoli, E., Meckler, A.N., Ziegler, M., Millan, I.M., Kluge, T., Deák, J., Hanselmann, K., John, C.M., 2015. Temperature dependence of oxygen-and clumped isotope fractionation in carbonates: a study of travertines and tufas in the 6–95°C temperature range. Geochimica et Cosmochimica Acta 168, 172-192.

Kelson, J.R., Huntington, K.W., Schauer, A.J., Saenger, C., Lechler, A.R., 2017. Toward a universal carbonate clumped isotope calibration: Diverse synthesis and preparatory methods suggest a single temperature relationship. Geochimica et Cosmochimica Acta 197, 104-131.

Kim, S.-T., Mucci, A., Taylor, B.E., 2007. Phosphoric acid fractionation factors for calcite and aragonite between 25 and 75°C: revisited. Chemical Geology 246, 135-146.

Kim, S.-T., O'Neil, J.R., 1997. Equilibrium and nonequilibrium oxygen isotope effects in synthetic carbonates. Geochimica et cosmochimica acta 61, 3461-3475.

Leng, M.J., Marshall, J.D., 2004. Palaeoclimate interpretation of stable isotope data from lake sediment archives. Quaternary Science Reviews 23, 811-831.

Li, H., Liu, X., Tripati, A., Feng, S., Kelley, A.M., 2020. Factors controlling the oxygen isotopic

composition of lacustrine authigenic carbonates in Western China: implications for paleoclimate reconstructions. Scientific Reports 10.

Liu, W., Zhang, P., Zhao, C., Wang, H., An, Z., Liu, H., 2018. Reevaluation of carbonate concentration and oxygen isotope records from Lake Qinghai, the northeastern Tibetan Plateau. Quaternary international 482, 122-130.

Liu, X., Dong, H., Rech, J.A., Matsumoto, R., Yang, B., Wang, Y., 2008. Evolution of Chaka Salt Lake in NW China in response to climatic change during the Latest Pleistocene–Holocene. Quaternary Science Reviews 27, 867-879.

Ma, R., Yang, G., Duan, H., Jiang, J., Wang, S., Feng, X., Li, A., Kong, F., Xue, B., Wu, J., 2011. China's lakes at present: number, area and spatial distribution. Science China Earth Sciences 54, 283-289.

Massey, J.F.J., 1951. The Kolmogorov-Smirnov Test for Goodness of Fit. Publications of the American Statistical Association 46, 68-78.

McCrea, J.M., 1950. On the isotopic chemistry of carbonates and a paleotemperature scale. The Journal of Chemical Physics 18, 849-857.

Meinicke, N., Ho, S., Hannisdal, B., Nürnberg, D., Tripati, A., Schiebel, R., Meckler, A., 2020. A robust calibration of the clumped isotopes to temperature relationship for foraminifers. Geochimica et Cosmochimica Acta 270, 160-183.

Mering, J., K, 2015. New constraints on water temperature at Lake Bonneville from carbonate clumped isotopes, Doctoral dissertation. University of California, Los Angeles.

Meyer, H.W., 2007. A review of paleotemperature–lapse rate methods for estimating paleoelevation from fossil floras. Reviews in Mineralogy and Geochemistry 66, 155-171.

778 Millero, F.J., Graham, T.B., Huang, F., Bustos-Serrano, H., Pierrot, D., 2006. Dissociation constants of
779 carbonic acid in seawater as a function of salinity and temperature. Marine Chemistry 100,
780 80-94.
781 Müller, I.A., Rodriguez-Blanco, J.D., Storck, J.C., Nascimento, G.S.D., Bernasconi, S.M., 2019.
782 Calibration of the oxygen and clumped isotope thermometers for (proto-)dolomite based on
783 synthetic and natural carbonates. Chemical Geology 525, 1-17.
784 Olack, G., Colman, A.S., 2019. Modeling the measurement: Δ_{47}, corrections and absolute ratios for
785 reference materials. Geochemistry, Geophysics, Geosystems 20, 3569-3587.
786 Passey, B.H., Henkes, G.A., 2012. Carbonate clumped isotope bond reordering and geospeedometry.
787 Earth & Planetary Science Letters 351-352, 223-236.
788 Petersen, S., Defliese, W., Saenger, C., Daëron, M., Huntington, K., John, C., Kelson, J., Bernasconi, S.,
789 Coleman, A., Kluge, T., 2019. Effects of Improved ^{17}O Correction on Inter-Laboratory
790 Agreement in Clumped Isotope Calibrations, Estimates of Mineral-Specific Offsets, and
791 Temperature Dependence of Acid Digestion Fractionation. Geochemistry, Geophysics,
792 Geosystems 20, 3495-3519.
793 Petryshyn, V., Lim, D., Laval, B., Brady, A., Slater, G., Tripati, A., 2015. Reconstruction of limnology
794 and microbialite formation conditions from carbonate clumped isotope thermometry.
795 Geobiology 13, 53-67.
796 Petryshyn, V.A., Rivera, M.J., Agić, H., Frantz, C.M., Corsetti, F.A., Tripati, A.E., 2016. Stromatolites
797 in Walker Lake (Nevada, Great Basin, USA) record climate and lake level changes~ 35,000
798 years ago. Palaeogeography, palaeoclimatology, palaeoecology 451, 140-151.
799 Santi, L., Arnold, A.J., Ibarra, D.E., Whicker, C., Tripati, A., 2020. Clumped isotope constraints on

changes in latest Pleistocene hydroclimate in the northwestern Great Basin: Lake Surprise, California. Geological Society of America Bulletin 132, 11-12.

Stolper, D.A., Eiler, J.M., 2015. The kinetics of solid-state isotope-exchange reactions for clumped isotopes: A study of inorganic calcites and apatites from natural and experimental samples. American Journal of Science 315, 363-411.

Sun, Q., Chu, G., Xie, M., Zhu, Q., Su, Y., Wang, X., 2018. An oxygen isotope record from Lake Xiarinur in Inner Mongolia since the last deglaciation and its implication for tropical monsoon change. Global and planetary change 163, 109-117.

Swart, Peter, K., Staudigel, Philip, T., 2016. Isotopic behavior during the aragonite-calcite transition: Implications for sample preparation and proxy interpretation. Chemical Geology 442, 130-138.

Tang, J., Dietzel, M., Fernandez, A., Tripati, A.K., Rosenheim, B.E., 2014. Evaluation of kinetic effects on clumped isotope fractionation (Δ_{47}) during inorganic calcite precipitation. Geochimica et Cosmochimica Acta 134, 120-136.

Thiagarajan, N., Adkins, J., Eiler, J., 2011. Carbonate clumped isotope thermometry of deep-sea corals and implications for vital effects. Geochimica et Cosmochimica Acta 75, 4416-4425.

Tripati, A.K., Eagle, R.A., Thiagarajan, N., Gagnon, A.C., Bauch, H., Halloran, P.R., Eiler, J.M., 2010. ^{13}C–^{18}O isotope signatures and 'clumped isotope'thermometry in foraminifera and coccoliths. Geochimica et cosmochimica acta 74, 5697-5717.

Tripati, A.K., Hill, P.S., Eagle, R.A., Mosenfelder, J.L., Tang, J., Schauble, E.A., Eiler, J.M., Zeebe, R.E., Uchikawa, J., Coplen, T.B., 2015. Beyond temperature: Clumped isotope signatures in dissolved inorganic carbon species and the influence of solution chemistry on carbonate

mineral composition. Geochimica et Cosmochimica Acta 166, 344-371.

Újvári, G., Kele, S., Bernasconi, S.M., Haszpra, L., Novothny, Á., Bradák, B., 2019. Clumped isotope paleotemperatures from MIS 5 soil carbonates in southern Hungary. Palaeogeography, palaeoclimatology, palaeoecology 518, 72-81.

Urey, H.C., 1947. The thermodynamic properties of isotopic substances. Journal of the Chemical Society, 562-581.

Watkins, J., Hunt, J., 2015. A process-based model for non-equilibrium clumped isotope effects in carbonates. Earth and Planetary Science Letters 432, 152-165.

Wen, Z., Mian-Ping, Z., Xian-Zhong, X., Xi-Fang, L., Gan-Lin, G., Zhi-Hui, H., 2005. Biological and ecological features of saline lakes in northern Tibet, China. Hydrobiologia 541, 189-203.

Yan, D., Wunnemann, B., 2014. Late Quaternary water depth changes in Hala Lake, northeastern Tibetan Plateau, derived from ostracod assemblages and sediment properties in multiple sediment records. Quaternary Science Reviews 95, 95-114.

Yang, W., Zuo, R., Wang, X., Song, Y., Jiang, Z., Luo, Q., Zhai, J., Wang, Q., Zhang, C., Zhang, Z., 2019. Sensitivity of lacustrine stromatolites to Cenozoic tectonic and climatic forcing in the southern Junggar Basin, NW China: New insights from mineralogical, stable and clumped isotope compositions. Palaeogeography, Palaeoclimatology, Palaeoecology 514, 109-123.

Yang, X., Scuderi, L., Paillou, P., Liu, Z., Li, H., Ren, X., 2011. Quaternary environmental changes in the drylands of China–A critical review. Quaternary Science Reviews 30, 3219-3233.

Zaarur, S., Olack, G., Affek, H.P., 2011. Paleo-environmental implication of clumped isotopes in land snail shells. Geochimica et Cosmochimica Acta 75, 6859-6869.

Zhai, D., Xiao, J., Fan, J., Wen, R., Pang, Q., 2015. Differential transport and preservation of the instars

of Limnocythere inopinata (Crustacea, Ostracoda) in three large brackish lakes in northern China. Hydrobiologia 747, 1-18.

Zhai, J., Wang, X., Qin, B., Cui, L., Zhang, S., Ding, Z., 2019. Clumped isotopes in land snail shells over China: Towards establishing a biogenic carbonate paleothermometer. Geochimica et Cosmochimica Acta 257, 68-79.

Zhang, G., Yao, T., Xie, H., Qin, J., Ye, Q., Dai, Y., Guo, R., 2014. Estimating surface temperature changes of lakes in the Tibetan Plateau using MODIS LST data. Journal of Geophysical Research: Atmospheres 119, 8552-8567.

Zhang, J., Ma, X., Qiang, M., Huang, X., Li, S., Guo, X., Henderson, A.C., Holmes, J.A., Chen, F., 2016. Developing inorganic carbon-based radiocarbon chronologies for Holocene lake sediments in arid NW China. Quaternary Science Reviews 144, 66-82.

Zhou, A., Chen, F., Qiang, M., Yang, M., Zhang, J., 2007. The discovery of annually laminated sediments (varves) from shallow Sugan Lake in inland arid China and their paleoclimatic significance. Science in China Series D: Earth Sciences 50, 1218-1224.

Figures

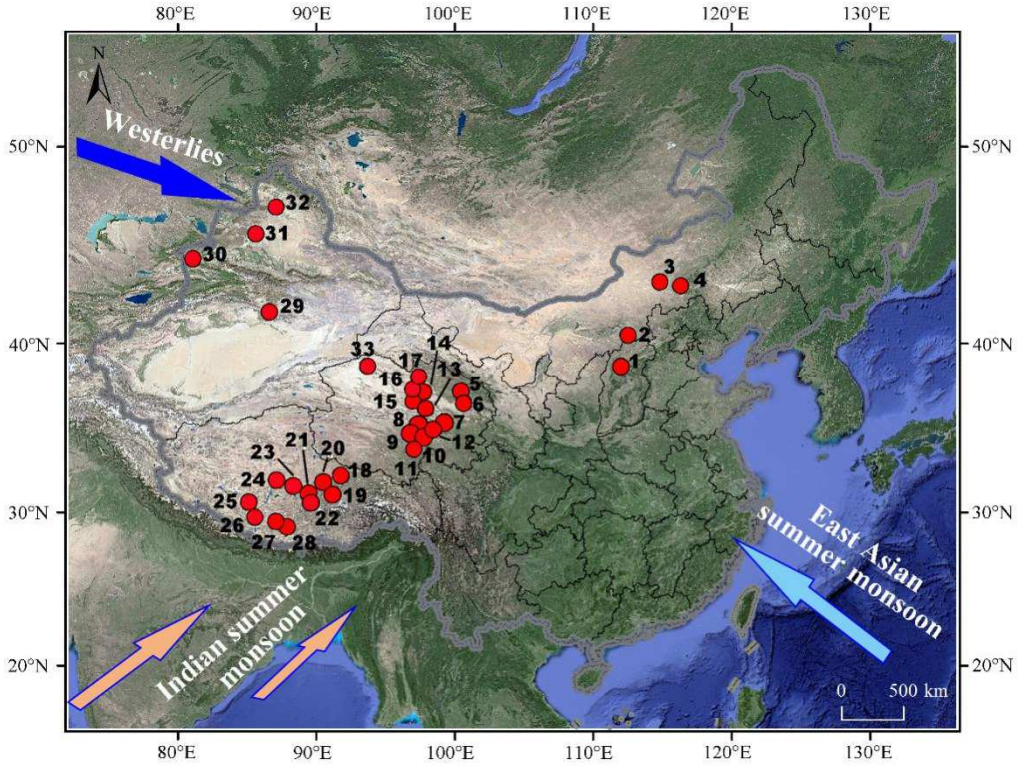

Fig. 1 Locations of where lacustrine sediments and water samples were collected from China. Corresponding numbers and lake names are listed in Table A. 1.

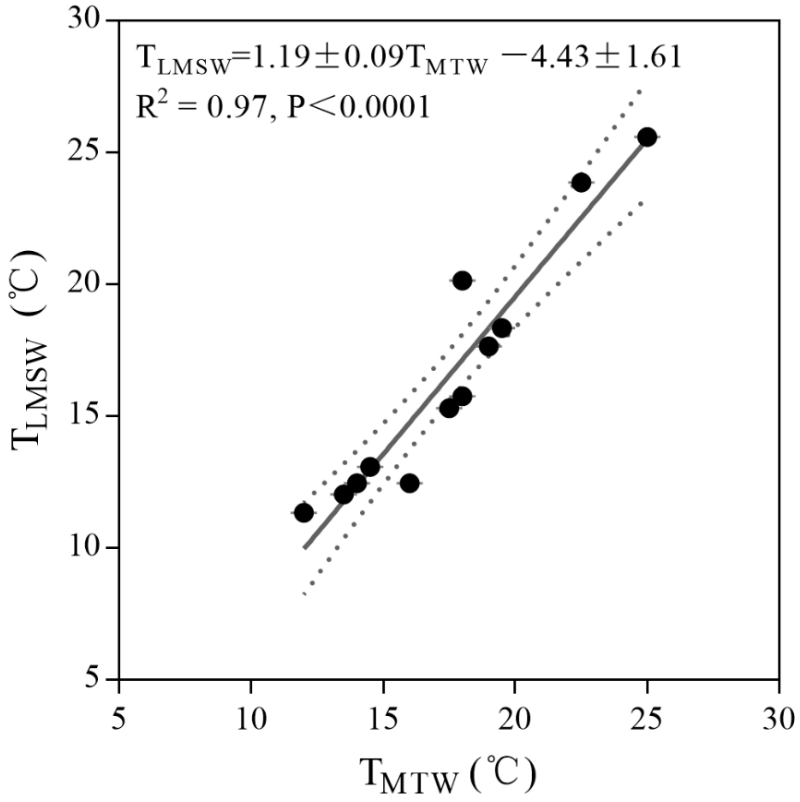

862

863 Fig. 2 Regression between midday temporal water temperature (T_{MTW}) and logged
864 mean summer water temperature (T_{LMSW}) showing a significant correlation.
865 Calculated mean summer water temperature (T_{CMSW}) was calculated using the
866 regression formula: $T_{CMSW} = 1.19 \pm 0.09T_{MTW} - 4.43 \pm 1.61$ ($R^2 = 0.91$, $P < 0.0001$, n
867 = 12). The dotted lines show 95% confidence intervals.

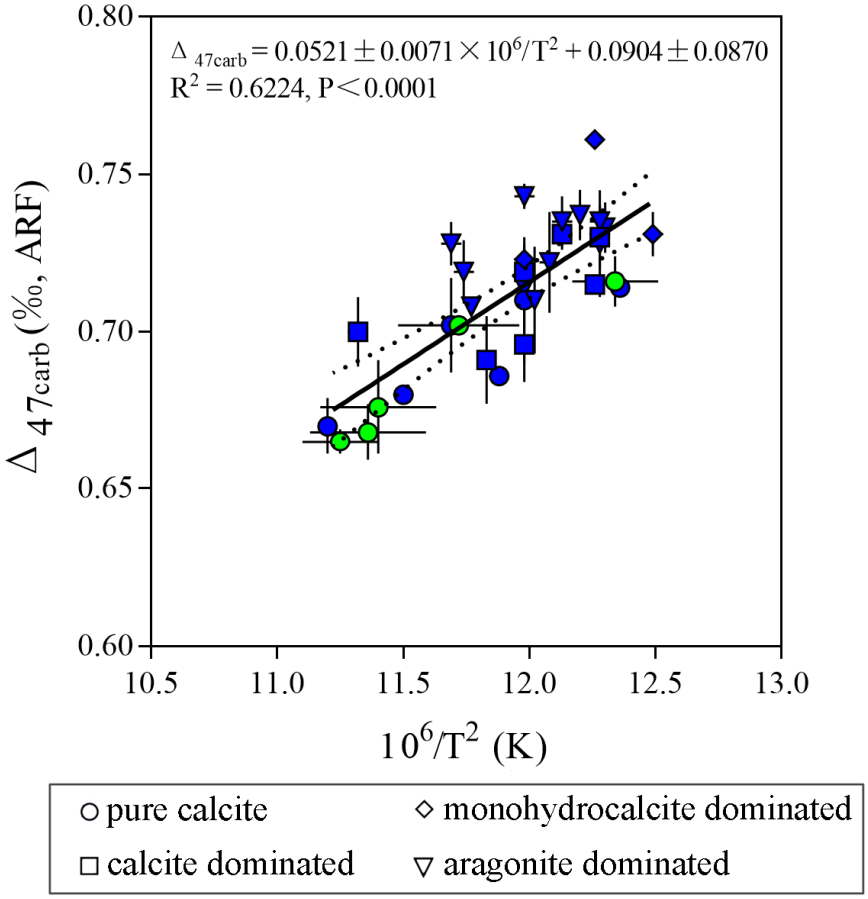

868

869 Fig. 3 Correlation between clumped isotope composition of modern lacustrine
870 authigenic carbonate (Δ_{47carb}) and independently measured lake mean summer water
871 surface temperature (T_{water}). The solid line is the least-squares linear regression line.
872 The dotted lines show 95% confidence intervals. Samples collected primarily from
873 Western China are marked in blue, while reprocessed data of 5 calcite micrites
874 collected from closed/dry lakes in China, the United States and Mexico are marked in
875 green. (For interpretation of the references to color in this figure legend, the reader is
876 referred to the web version of this article.)

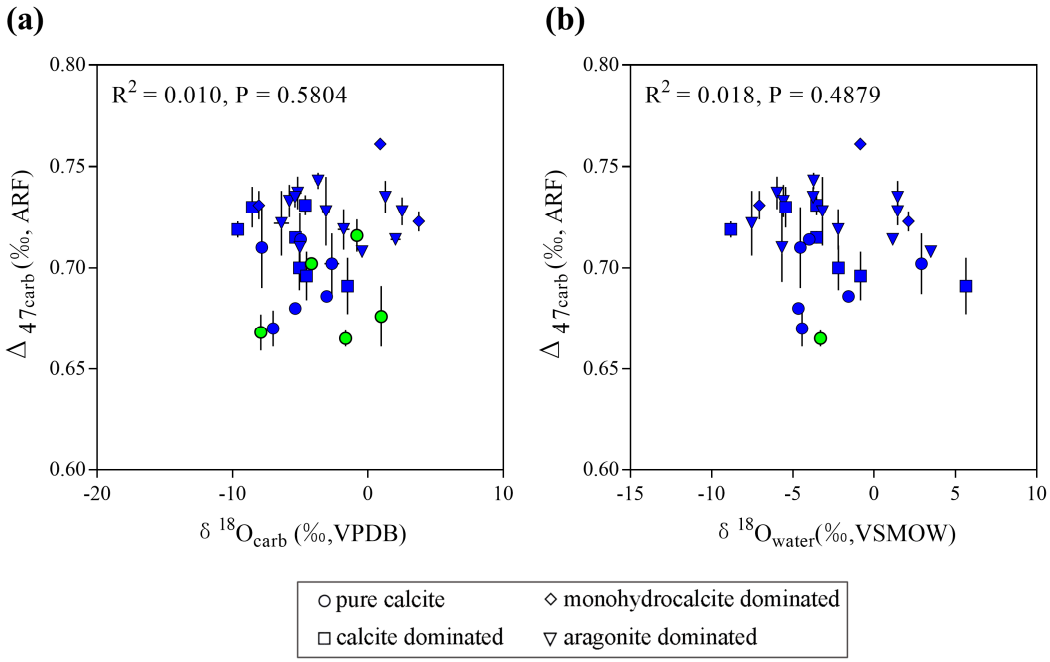

877

878 Fig. 4 No statistically significant correlation is observed neither between (a) $\delta^{18}O_{carb}$

879 and Δ_{47carb} (R^2 = 0.010, P = 0.5804); nor between (b) $\delta^{18}O_{water}$ and Δ_{47carb} (R^2 = 0.018,

880 P = 0.4879). Samples collected from China are marked in blue, while reprocessed data

881 of 5 calcite micrites collected from closed/dry lakes in China, the United States and

882 Mexico are marked in green. (For interpretation of the references to color in this

883 figure legend, the reader is referred to the web version of this article.)

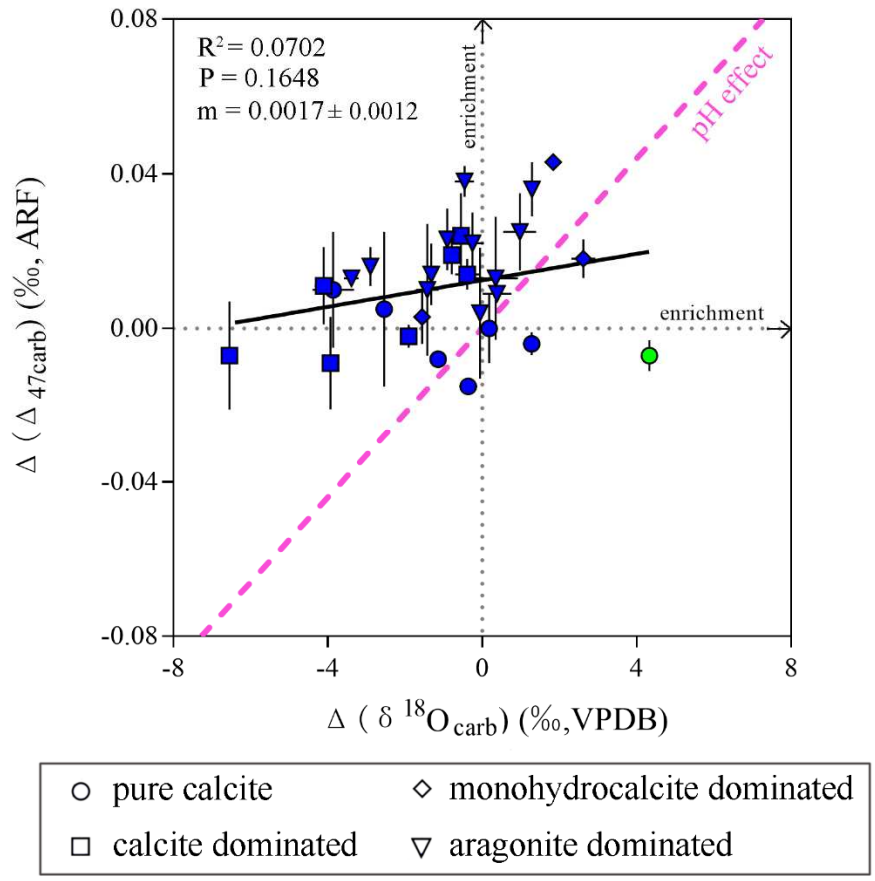

884

885 Fig. 5 Deviations of measured from expected $\delta^{18}O_{carb}$ ($\Delta(\delta^{18}O_{carb})$) and that of
886 measured from predicted Δ_{47carb} ($\Delta(\Delta_{47carb})$) based on the calibrations of Bernasconi et
887 al. (2018) and Kim and O'Neil (1997) for lacustrine authigenic carbonates. The pink
888 dashed line (m = 0.011) indicates deviations expected for changes in water pH (Tripati
889 et al., 2015). If carbonates are affected by pH-related speciation, the slope of
890 $\Delta(\delta^{18}O)$-$\Delta(\Delta_{47})$ would be close to 0.011 ± 0.001 (Tripati et al., 2015). However, the
891 correlation between $\Delta(\delta^{18}O_{carb})$ and $\Delta(\Delta_{47carb})$ is not significant for modern lacustrine
892 authigenic carbonates in this study. The slope of $\Delta(\delta^{18}O_{carb})$-$\Delta(\Delta_{47carb})$ is 0.0017 ±
893 0.0012. Samples collected from China are marked in blue, while reprocessed data of 5

894 calcite micrites collected from closed/dry lakes in China, the United States and
895 Mexico are marked in green. (For interpretation of the references to color in this
896 figure legend, the reader is referred to the web version of this article.)

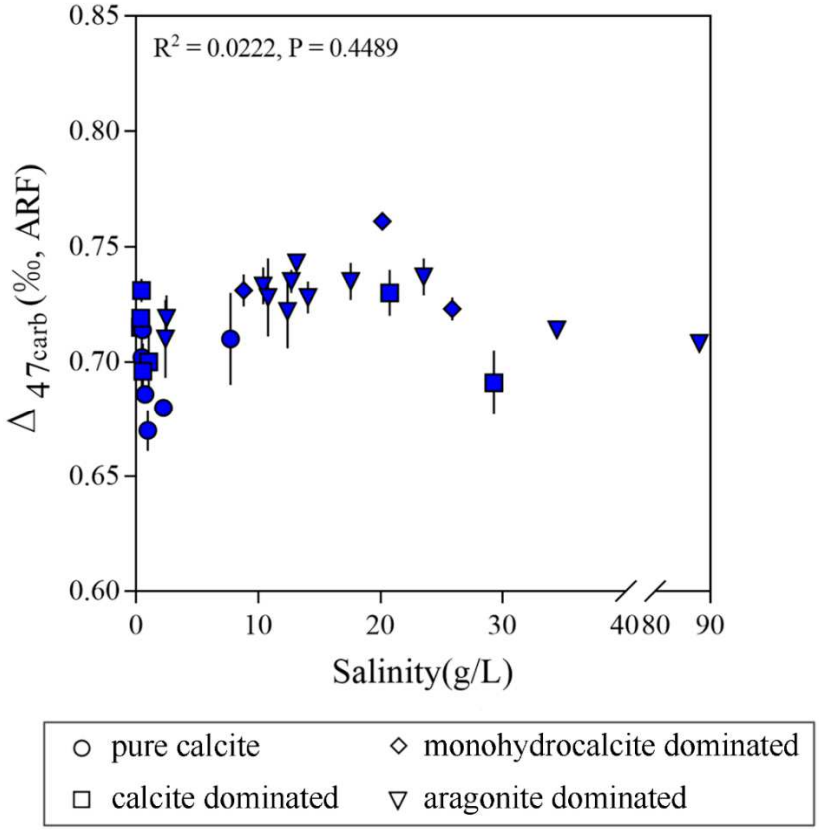

897

898 Fig. 6 Comparison between Δ_{47carb} values and water salinity of 28 lakes located in

899 China. No statistically significant linear correlation is observed between Δ_{47carb} and

900 lake water salinity (R^2 = 0.0222, P = 0.4489).

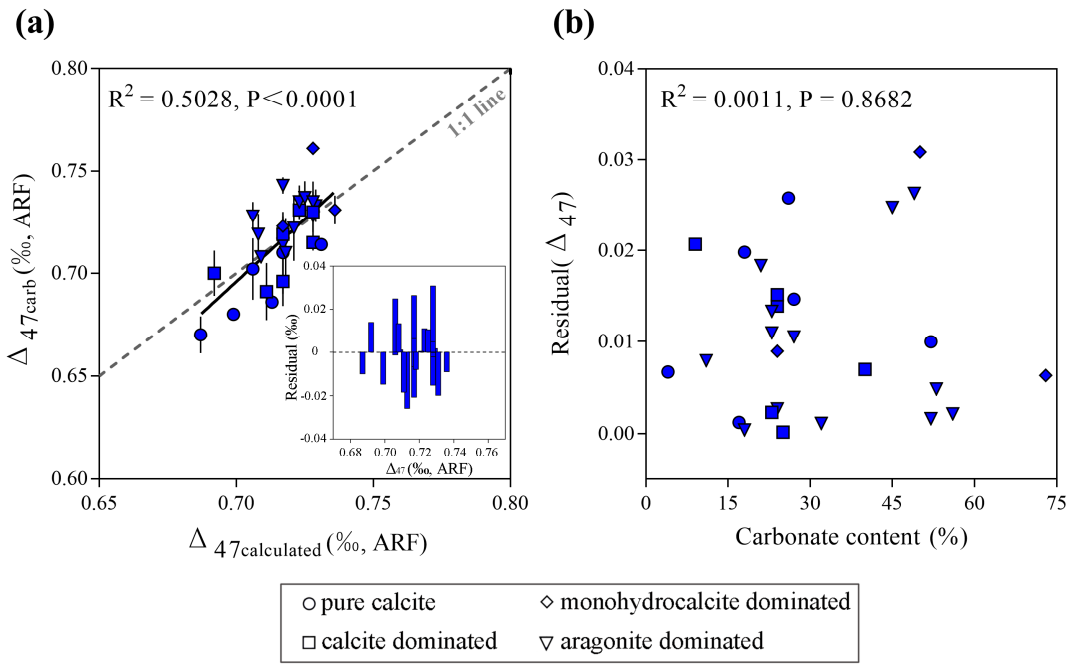

901

902 Fig. 7 Comparison between (a) Δ_{47carb} and $\Delta_{47calculated}$, and that between (b) Δ_{47}

903 residual and carbonate content of 28 lakes located in China. There is no significant

904 correlation between Δ_{47} residual and carbonate content (R^2 = 0.00118, P = 0.8682).

905 The dashed line is a 1:1 line.

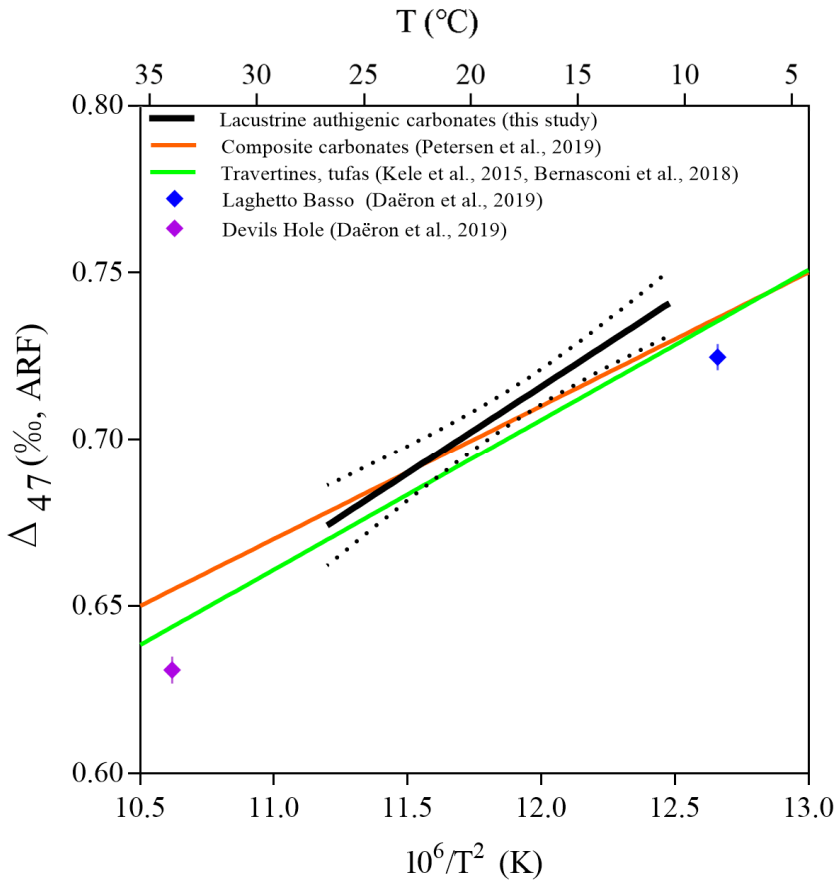

906

907 Fig. 8 Comparison of carbonate Δ_{47}–temperature calibrations with the recalculated
908 Kele et al. (2015) calibration (Bernasconi et al., 2018), a composite calibration line
909 from Petersen et al. (2019), and slowly precipitated calcites from Devils Hole and
910 Laghetto Basso (Daëron et al., 2019). The black solid line represents a linear
911 least-squares regression based on mean Δ_{47} values of modern lacustrine authigenic
912 carbonates from this study. The dotted lines show 95% confidence intervals. All
913 calibrations are corrected by IUPAC parameters (Brand et al., 2010). (For
914 interpretation of the references to color in this figure legend, the reader is referred to
915 the web version of this article.)

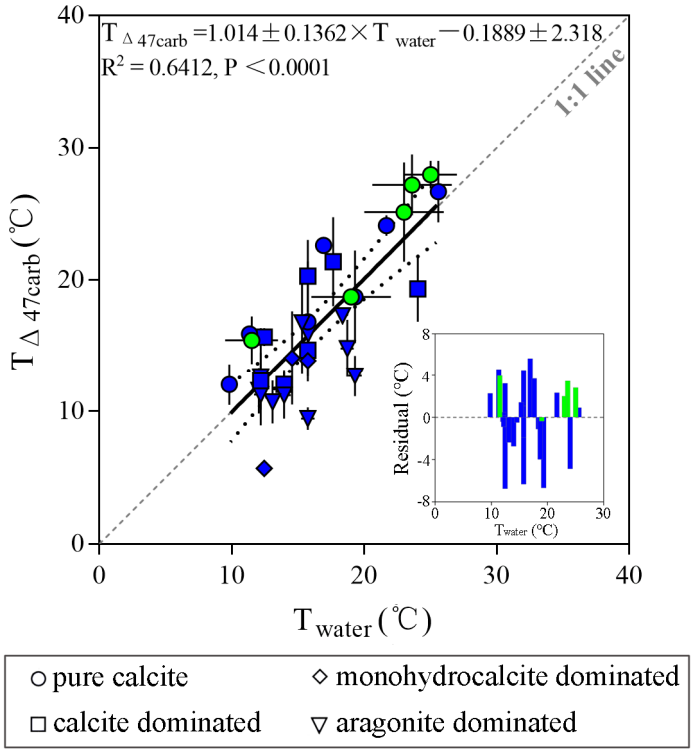

Fig. 9 Comparison between independently measured lake mean summer water surface temperatures (T_{water}) and Δ_{47} recorded temperatures that calculated by lacustrine authigenic carbonates ($T_{\Delta 47carb}$) calculated using Eq. 2 in this study. The dotted lines represent the 95% confidence intervals. The dashed line is 1:1 line. Samples collected from China are marked in blue, while reprocessed data of 5 calcite micrites collected from closed/dry lakes in China, the United States and Mexico are marked in green. (For interpretation of the references to color in this figure legend, the reader is referred to the web version of this article.)

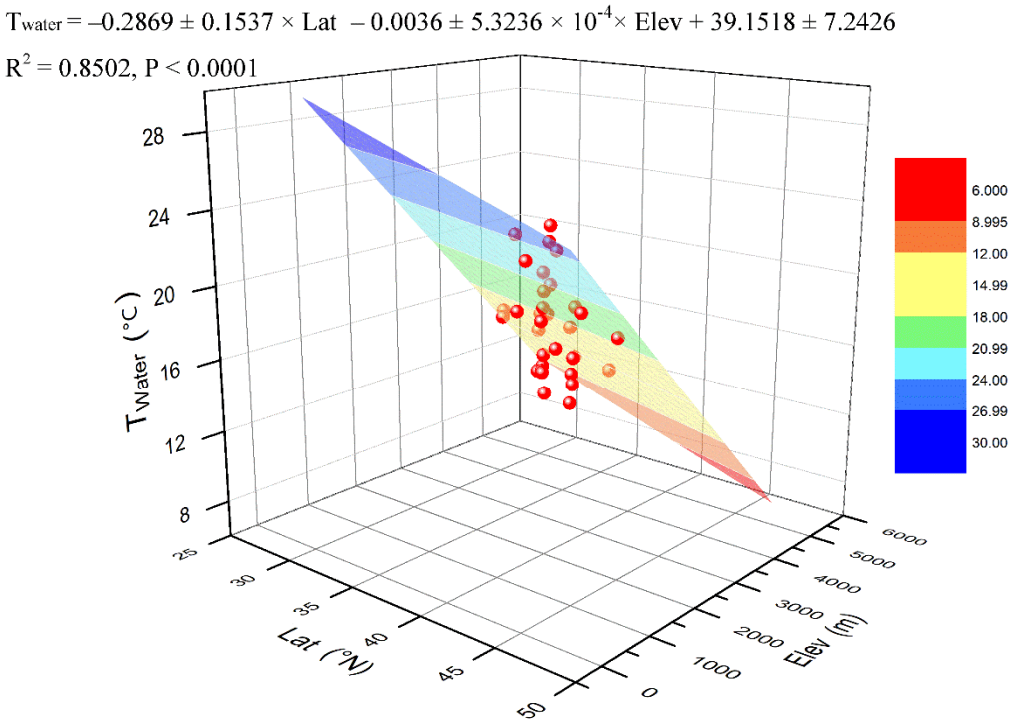

925

926 Fig. 10 Combined effects of lake latitude (Lat) and elevation (Elev) on independently

927 measured lake mean summer water surface temperature (T_{water}) for the 33 lakes

928 located in China. (For interpretation of the references to color in this figure legend,

929 the reader is referred to the web version of this article.)

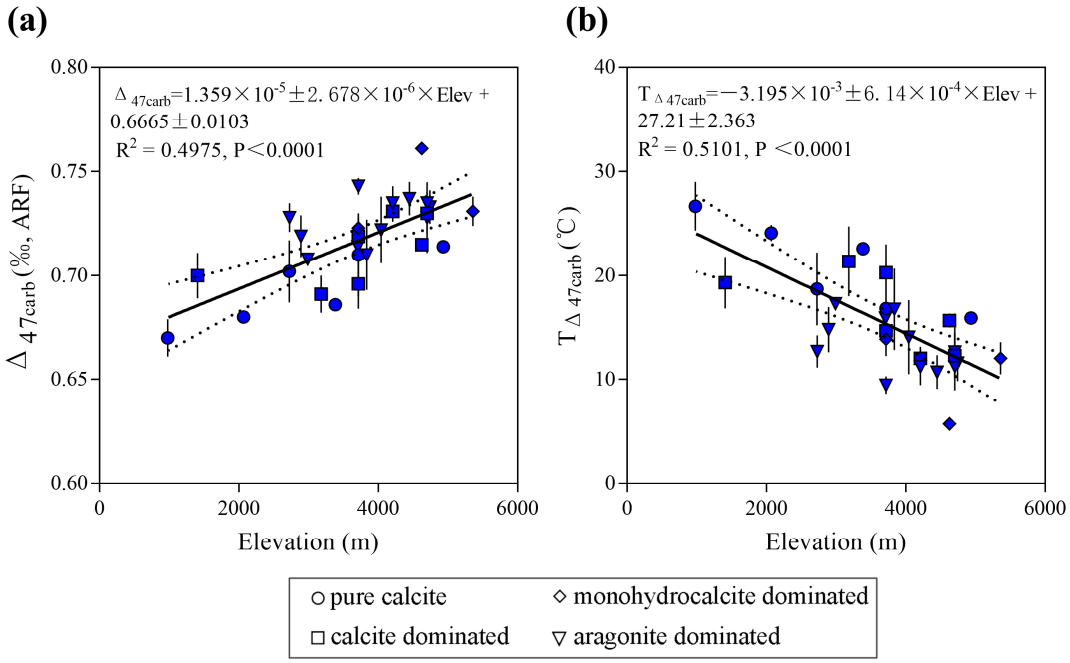

930

931 Fig. 11 Comparison between (a) lake elevation (Elev) and Δ_{47carb}; (b) lake elevation
932 (Elev) and $T_{\Delta 47carb}$ that calculated using Eq. 2 in this study. The solid lines are the
933 least-squares linear regression lines. In this case, lake elevations are recalculated
934 based on the Eq. 4 assuming all lakes located at 35°N, which is a mean value of the
935 latitude gradient of the 28 lakes located in China. The dotted lines show 95%
936 confidence intervals.

Figure Captions

Fig. 1 Locations of where lacustrine sediments and water samples were collected from China. Corresponding numbers and lake names are listed in Table A. 1.

Fig. 2 Regression between midday temporal water temperature (T_{MTW}) and logged mean summer water temperature (T_{LMSW}) showing a significant correlation. Calculated mean summer water temperature (T_{CMSW}) was calculated using the regression formula: $T_{CMSW} = 1.19 \pm 0.09 T_{MTW} - 4.43 \pm 1.61$ ($R^2 = 0.91$, $P < 0.0001$, $n = 12$). The dotted lines show 95% confidence intervals.

Fig. 3 Correlation between clumped isotope composition of modern lacustrine authigenic carbonate (Δ_{47carb}) and independently measured lake mean summer water surface temperature (T_{water}). The solid line is the least-squares linear regression line. The dotted lines show 95% confidence intervals. Samples collected primarily from Western China are marked in blue, while reprocessed data of 5 calcite micrites collected from closed/dry lakes in China, the United States and Mexico are marked in green. (For interpretation of the references to color in this figure legend, the reader is referred to the web version of this article.)

Fig. 4 No statistically significant correlation is observed neither between (a) $\delta^{18}O_{carb}$ and Δ_{47carb} ($R^2 = 0.010$, $P = 0.5804$); nor between (b) $\delta^{18}O_{water}$ and Δ_{47carb} ($R^2 = 0.018$, $P = 0.4879$). Samples collected from China are marked in blue, while reprocessed data

of 5 calcite micrites collected from closed/dry lakes in China, the United States and Mexico are marked in green. (For interpretation of the references to color in this figure legend, the reader is referred to the web version of this article.)

Fig. 5 Deviations of measured from expected $\delta^{18}O_{carb}$ ($\Delta(\delta^{18}O_{carb})$) and that of measured from predicted Δ_{47carb} ($\Delta(\Delta_{47carb})$) based on the calibrations of Bernasconi et al. (2018) and Kim and O'Neil (1997) for lacustrine authigenic carbonates. The pink dashed line (m = 0.011) indicates deviations expected for changes in water pH (Tripati et al., 2015). If carbonates are affected by pH-related speciation, the slope of $\Delta(\delta^{18}O)$-$\Delta(\Delta_{47})$ would be close to 0.011 ± 0.001 (Tripati et al., 2015). However, the correlation between $\Delta(\delta^{18}O_{carb})$ and $\Delta(\Delta_{47carb})$ is not significant for modern lacustrine authigenic carbonates in this study. The slope of $\Delta(\delta^{18}O_{carb})$-$\Delta(\Delta_{47carb})$ is 0.0017 ± 0.0012. Samples collected from China are marked in blue, while reprocessed data of 5 calcite micrites collected from closed/dry lakes in China, the United States and Mexico are marked in green. (For interpretation of the references to color in this figure legend, the reader is referred to the web version of this article.)

Fig. 6 Comparison between Δ47carb values and water salinity of 28 lakes located in China. No statistically significant linear correlation is observed between Δ47carb and lake water salinity (R2 = 0.0222, P = 0.4489).

Fig. 7 Comparison between (a) Δ_{47carb} and $\Delta_{47calculated}$, and that between (b) Δ_{47} residual and carbonate content of 28 lakes located in China. There is no significant correlation between Δ_{47} residual and carbonate content (R^2 = 0.00118, P = 0.8682). The dashed line is a 1:1 line.

Fig. 8 Comparison of carbonate Δ_{47}–temperature calibrations with the recalculated Kele et al. (2015) calibration (Bernasconi et al., 2018), a composite calibration line from Petersen et al. (2019), and slowly precipitated calcites from Devils Hole and Laghetto Basso (Daëron et al., 2019). The black solid line represents a linear least-squares regression based on mean Δ_{47} values of modern lacustrine authigenic carbonates from this study. The dotted lines show 95% confidence intervals. All calibrations are corrected by IUPAC parameters (Brand et al., 2010). (For interpretation of the references to color in this figure legend, the reader is referred to the web version of this article.)

Fig. 9 Comparison between independently measured lake mean summer water surface temperatures (T_{water}) and Δ_{47} recorded temperatures that calculated by lacustrine authigenic carbonates ($T_{\Delta47carb}$) calculated using Eq. 2 in this study. The dotted lines represent the 95% confidence intervals. The dashed line is 1:1 line. Samples collected from China are marked in blue, while reprocessed data of 5 calcite micrites collected from closed/dry lakes in China, the United States and Mexico are marked in green.

(For interpretation of the references to color in this figure legend, the reader is referred to the web version of this article.)

Fig. 10 Combined effects of lake latitude (Lat) and elevation (Elev) on independently measured lake mean summer water surface temperature (T_{water}) for the 33 lakes located in China. (For interpretation of the references to color in this figure legend, the reader is referred to the web version of this article.)

Fig. 11 Comparison between (a) lake elevation (Elev) and Δ47carb; (b) lake elevation (Elev) and TΔ47carb that calculated using Eq. 2 in this study. The solid lines are the least-squares linear regression lines. In this case, lake elevations are recalculated based on the Eq. 4 assuming all lakes located at 35°N, which is a mean value of the latitude gradient of the 28 lakes located in China. The dotted lines show 95% confidence intervals.